



## Bioactive studies of TiO<sub>2</sub> nanoparticles synthesized using *Glycyrrhiza glabra*

Muthiah Bavanilatha\*, Lakshmanan Yoshitha, S. Nivedhitha, S. Sahithya

Department of Biotechnology, Sathyabama Institute of Science and Technology, Jeppiaar Nagar, Raajiv Gandhi Salai, Chennai, Tamil Nadu, 600 119, India

### ARTICLE INFO

#### Keywords:

Titanium dioxide  
Licorice  
SEM  
FTIR  
Nanoparticles  
Antibacterial  
Anticancer

### ABSTRACT

The world is fascinated by the emergence of nano products with the venture of nanotechnology with indomitable scientific advancements in almost all domains. The most interesting aspect of nanomaterials involves its synthesis protocol using green chemistry principles. In the event of eco-friendly approach, TiO<sub>2</sub> nanoparticles were synthesized using *Glycyrrhiza glabra* root extracts from titanium oxy-sulfate precursor. These TiO<sub>2</sub> nanoparticles were characterized by means of spectroscopic and electron microscopic techniques. These nanoparticles showed maximum absorbance at 250 nm. The involvement of phytochemicals, proteins and their interaction in the nanoparticle formation was determined using Fourier Transform Infrared Spectroscopy (FTIR). X-ray diffraction (XRD) pattern was found to exhibit typical anatase phase of nano crystal possessing  $\zeta$  value of  $-31\text{mV}$ . Electron micrograph of TiO<sub>2</sub> NPs showed spherical shaped particles with an average size of 69 nm. TiO<sub>2</sub> Nanoparticles exhibited antibacterial activity against the tested microorganisms. The cytotoxic activity of the synthesized nanoparticles was evaluated by MTT assay and IC<sub>50</sub> values were found to be 1.25  $\mu\text{g}$  and 0.3125  $\mu\text{g}$  respectively against Vero and HEp2 cell lines. Biocompatibility studies were also carried out using zebra fish (*Danio rerio*) embryo model which proved that they are not cytotoxic to the embryo which is evident from their developmental stages. Such highly robust, stable, biocompatible TiO<sub>2</sub> Nanoparticles with potential biological activity prove to be a promising multifaceted therapeutic agent demanding *in vivo* studies.

### 1. Introduction

The field of nanotechnology is relatively a new discipline with huge applications in many areas including medicine (Nano medicine) and pharmacology industries and also considered to be one of the most active areas of research in modern materials science. Increased surface area, size and morphology are different characteristic properties of nanoparticles that are considered to be improved when compared to the bulk counterparts. Physical properties, chemical reactivity and potential applications in various research areas such as antibacterial, antiviral, diagnostics, anticancer and targeted drug delivery have led to the extensive exploitation of the metal nanoparticles (Paskalis et al., 2014).

The traditional methods for the metal nanoparticle synthesis are chemical reduction method, solvo-thermal reduction, electrochemical techniques and photochemical reaction in reverse micelles (Balantrapu and Goia, 2009; Taleb et al., 1997; Sharmila et al., 2014). Among which chemical reduction is the most frequently applied method, but the chemically synthesized nanoparticles were reported to have less stability and more agglomeration (Mukherjee et al., 2001) and the generated particles were larger in size and consumed more energy. Hence an attempt has been made to develop an eco-friendly protocol which could

produce dispersible and stable nanoparticles and also consume less energy.

The method that was repeatedly adopted for the metal and metal oxide nanoparticle synthesis called as Green Synthesis method, with bacteria, fungi and plant extract was not only a preliminary and user friendly but does not require much laboratory equipments and it was a rapid, cost effective easily scalable and more efficient than conventional method of synthesis. Bhainsa and D'Souza, 2006 and Willner et al. (2007) state that most of the methods utilized green synthesis for the preparation of nanoparticles with more dispersity, high stability and narrow size distribution.

Titanium dioxide is an n-type semiconductor with extensive range energy band gap in the pathway of photocatalytic activity. This ceramic material has three different structures: rutile, anatase and brookite (Murugan et al., 2006). Titanium dioxide is comprehensively used in the fabrication of core-shell systems as a photocatalytic agent because of its exceptional properties such as strong oxidation reaction, large effective surface area and low toxicity (Kong et al., 2010).

*Glycyrrhiza glabra* commonly referred to as Licorice is a perennial herb native to the Mediterranean region central to southern Russia, and Asia Minor to Iran, now widely cultivated throughout Europe, the

\* Corresponding author. Department of Biotechnology, Faculty of Bio & Chemical Engineering, Sathyabama Institute of Science & Technology, Jeppiaar Nagar, Raajiv Gandhi Salai, Chennai, 600 119, Tamil Nadu, India.

E-mail address: [bavagold@gmail.com](mailto:bavagold@gmail.com) (M. Bavanilatha).

<https://doi.org/10.1016/j.bcab.2019.101131>

Received 13 February 2018; Received in revised form 31 January 2019; Accepted 9 April 2019

Available online 16 April 2019

1878-8181/ © 2019 Published by Elsevier Ltd.

Middle East ((Blumenthal and Goldberga,2000), Southern Europe and parts of Asia such as India. It is used as medicine in various systems of medicine for its anti-allergy, anti-inflammatory, expectorant, spasmolytic, antiulcer activity (Khare, 2007). The root of the *Glycyrrhiza glabra* contains a sweet flavor Licorice, which can be extracted. *Glycyrrhiza* consists of about 30 species, which are used for treatment of acute and chronic poisonings, respiratory tract infections, dry cough & bronchitis (Esra I and Seno I,2000; Kreyling et al., 2002). The extracts of Licorice are also used as flavoring and sweetening agents in chewing gums, candies, sweets, toothpastes and beverages. Glycyrrhizin, Glabranin A and B, Glycyrrhetol, Glabridin, Formononetin, Glabrone, etc are the major bioactive constituents of *G. glabra*.

In the present study, *Glycyrrhiza glabra* roots were used for the synthesis of TiO<sub>2</sub> nanoparticles and its biological and anticancer effects *in vitro* using Vero and HEP-2 (Laryngeal epidermoid carcinoma, a common malignant tumor of head and neck) cell lines have been investigated. Moreover, the biocompatibility of green synthesized TiO<sub>2</sub> nanoparticles has also been studied using zebra fish embryo.

## 2. Materials and methods

### 2.1. Materials

The roots of *G. glabra* were purchased from a local market in Chennai. The chemicals and reagents used for the synthesis were purchased from Southern India Chemicals, Chennai and Sigma Aldrich, St. Louis, USA. The cell culture medium, growth factor and its supplements were purchased from Hi media, India. The Human Laryngeal carcinoma cell line (HEP-2) and Vero (African green monkey kidney epithelial) cell lines procured from National Centre for Cell Science (NCCS), Pune, India, were maintained in 5% CO<sub>2</sub> incubator.

### 2.2. Preparation of aqueous extract of *G. glabra*

*G. glabra* root sample was air dried and ground into fine powder. 5 g of sample was dissolved in distilled water and heated to 70° C for 2 min to get aqueous extracts. The obtained aqueous extract was used for the TiO<sub>2</sub> nanoparticle synthesis. The phytochemical analysis of aqueous extract was carried out to find out the presence of the phytochemicals such as alkaloids, saponin etc, (Hudlikar et al., 2012).

### 2.3. Synthesis of TiO<sub>2</sub> nanoparticles

The TiO<sub>2</sub> nanoparticles were synthesized using previously published methodology in which TiO<sub>2</sub> precursor was reduced and stabilized by the phytochemicals present in the bacterial culture filtrate (Valli et al., 2016). For nanoparticle synthesis, 100 ml of titanium oxysulfate (0.5 M) was heated to 50° C and 5 ml of aqueous root extract was added to the solution under continuous stirring on a magnetic stirrer. The mixture was kept under stirring condition until the formation of white precipitate (Swetha et al., 2014; Valli et al., 2016). This milky white precipitate was collected and dried in a hot air oven at 60 °C overnight and the obtained nanoparticle was used for further experiments.

### 2.4. Characterization of TiO<sub>2</sub> nanoparticles

Characterization studies of the nanoparticles provide an idea on the dispersive nature, crystalline structure and in prompt precise approach involved in nanoparticle synthesis. UV-vis spectroscopic analysis (UV-1600, Shimadzu, Japan) of the phytosynthesized TiO<sub>2</sub> nanoparticles was carried out (Ching Song et al 2005). The role of the root extract as a reducing and stabilizing agent in the event of nanoparticle synthesis was evaluated using Fourier Transform Infrared spectroscopy (FTIR) using FTIR 4400 PerkinElmer model in the mid-infrared region (MIR) within the range of 400–4000 cm<sup>-1</sup>. In addition, the morphological features of TiO<sub>2</sub> NPs were recorded using the Carl Zeiss FESEM-SUPRA

55 microscope. X-ray diffraction (XRD) pattern of . TiO<sub>2</sub> nanoparticle was obtained using a X-ray diffractometer Phillips® PW 1830 model with CuKα radiation at 2θ in the range of 20–80° (λ = 0.154 nm). For zeta potential measurements, 0.01 g of the sample was suspended in 1000 μl of sterile deionised water. The Zetasizer Nano ZS particle system from Malvern Instruments was used to measure the zeta potential (ξ) of TiO<sub>2</sub> NPs.

### 2.5. Antibacterial activity of TiO<sub>2</sub> NPs

The antibacterial activity of the phytosynthesized TiO<sub>2</sub> NPs was assessed using Kirby Bauer's agar diffusion method against gram positive *Staphylococcus aureus* and gram negative *Klebsiella pneumoniae*. Ciprofloxacin was used as positive control. TiO<sub>2</sub> NPs at different concentrations viz., 5, 2.5, 1.25, 0.63 and 0.312 μg/ml was prepared using deionised water and subjected to antimicrobial sensitivity testing. Log phase cultures of the above mentioned cultures were suspended in sterile saline and swabbed over the Muller Hinton Agar (MHA) medium using a sterile swab. The agar medium was punched with a 3 mm gel puncture for loading different concentrations of NPs and incubated at 37 °C for 18–24 h. Prior to the incubation period the plates were observed for Zone of inhibition (ZOI) and the zone of inhibition was measured.

### 2.6. *In vitro* studies using cell lines

Vero and HEP-2 cell lines with 80% and more monolayer confluency were preferred for *in vitro* studies. Initially, the cells were seeded into 96 well plate so that the final concentration worked out to 1 × 10<sup>5</sup> cells per well. The plates were incubated at 37 °C under 5% CO<sub>2</sub> environment. A stock solution of TiO<sub>2</sub> NPs at 10 mg/ml concentration was prepared in 0.5% DMSO (w/v), vortexed and stored at 4 °C. Doubling dilutions i.e. 1:2, 1:4, 1:8, 1:16, 1:32, 1:64, 1:128 were made using MEM. The final concentration of DMSO in the culture medium was not more than 0.01% (v/v) and used as control. Prior to incubation, Vero and HEP2 cell lines were observed using an inverted microscope to assess the degree of confluency and the absence of bacterial and fungal contaminants.

#### 2.6.1. Cytotoxicity studies of TiO<sub>2</sub> nanoparticles

The *in vitro* toxicity studies on Vero and HEP-2 cells were determined using MTT (3–4,5 dimethyl thiazol-(2 yl) 2–5 diphenyltetrazolium bromide) assay (Mosmann, 1983 and Gupta and Gupta, 2004). The cells were treated with various concentrations of TiO<sub>2</sub> NPs (ranging from 5 mg to 0.0045 μg/ml) and incubated overnight at 37 °C for 24 h. After incubation period, the supernatant was removed and 20 μl of MTT (5 mg/ml) was added and incubated in dark condition for 4 h. Formazan crystals formed were solubilised using 180 μl of DMSO which simultaneously stop the reaction. The relative absorbance was recorded at 570 nm to determine the cell cytotoxicity using the formulae given below.

$$\% \text{ Cytotoxicity} = 1 - \left( \frac{\text{Absorbance of TiO}_2 \text{ NPs}}{\text{Absorbance of Control}} \right)$$

### 2.7. Biocompatibility of TiO<sub>2</sub> NPs using zebra fish model

The *in vivo* toxicity assessment and imaging was performed using zebra fish (*Danio rerio*, wild type, Tubingen) embryos (Bavanilatha et al., 2016 and Shasahank Chetty et al 2016). The adult male and female zebra fishes (1:4) were placed separately in breeding box maintained with controlled light and temperature conditions (26°C) with a 14hr/10 h light/dark cycle. The fishes were fed with dry flakes and nauplius larva once in a day. To prevent the eggs from cannibalism by the adult zebra fish the spawn traps were covered with a stainless steel mesh.

Spawning and fertilization was triggered within 30 min, once the light was turned on. The embryos were collected using a tea filter and washed 3 times with E3 Medium (5 mM NaCl 0.17 M KCl, 0.33 mM CaCl<sub>2</sub> and 0.33 mM MgSO<sub>4</sub>, pH 7.2 to 7.4) to remove the debris prior to analysis. The fertilized eggs undergo first cleavage after approximately 15 min and consecutive synchronous cleavages from 4, 8, 16 and 32 blastomeres. One day old healthy embryos were placed in 6 well culture plates (10 embryos/well in E3 medium of about 2 ml) and treated with different concentrations of TiO<sub>2</sub> NPs (1, 0.5, 2.5, 0.125, 0.0 63, 0.031 mg/ml). The untreated embryos in E3 medium served as control. The developmental stages of zebra fish embryos was observed from 15 min to 96th hour of treatment with TiO<sub>2</sub> nanoparticles using an Olympus bright field inverted microscope (CKX 14,USA).

### 3. Results and discussion

#### 3.1. UV-vis spectroscopic analysis

The root extract of *G. glabra* when mixed with the precursor molecule and the Nanoparticle formation was monitored by observing the formation of white precipitate. UV-visible spectra of the green synthesized TiO<sub>2</sub> nanoparticles showed a characteristic peak at approximately 250 nm ( $\lambda_{max}$ ) due to the surface plasmon resonance vibration in the reaction mixture. The optimized reaction conditions for TiO<sub>2</sub> NPs were as follows: 95 ml of 0.5 M Titanium oxy sulphate solution containing 5 ml root extract; temperature 37 °C; pH 7.4; reaction period, 4 h. The formation of milky white colloidal solution indicated the conversion of Titanium oxysulphate solution with the *glabra* extracts into nanosized TiO<sub>2</sub> nanoparticles (Fig. 1)

#### 3.2. Fourier Transform Infrared Spectroscopy

The FTIR spectroscopic tool revealed the chemical composition and bonding pattern of reducing and capping agents involved in NP synthesis Fig. 2 shows the FTIR spectra of the phytosynthesized TiO<sub>2</sub> nanoparticles using the aqueous root extract of *G. glabra*. The FTIR spectrum of TiO<sub>2</sub>NPs showed the presence of aromatic primary amine which is confirmed from the peaks corresponding to NH stretch (3414 cm<sup>-1</sup>), NH bending (1664 cm<sup>-1</sup>) and hydroxyl stretch (2360 cm<sup>-1</sup>) indicating the involvement of proteins in synthesis of nanoparticles (Rajakumar and Abdul, 2013). H The peaks 1543 and 1525 cm<sup>-1</sup> confirm the presence of benzene ring which forms the major

portions of flavonoids, phytosterols etc indicating the involvement of these compounds in the formation of TiO<sub>2</sub> nanoparticles. The occurrence of these peaks in the FT-IR spectrum evidently indicate the dual role of the *G. glabra* root extract as a green reducing agent and stabilizing agent as well (Rajakumar et al., 2012)

#### 3.3. XRD analysis of TiO<sub>2</sub> NPs

The typical X-ray diffractogram of phytosynthesized TiO<sub>2</sub> NPs showed relatively pronounced diffraction peaks when 2 $\theta$  is 24.34°, 49.80°, 65.11° and 80° corresponding to planes (110), (211), (112) and (220) Bragg reflections (JCPDS 90-08213) confirming the anatase phase of nanocrystal. While most of the biologically synthesized TiO<sub>2</sub> NPs were found to be predominantly in anatase crystal phase (Valli et al., 2016) rutile crystal phase was also reported (Barbe et al 2005 and Dongxu et al., 2013). The peaks are comparable with the standard peaks in COD DB Card number 90-08554. The average particle diameter of the nanoparticles was calculated from XRD pattern using the Scherer's equation:

$$D = \frac{0.9 \lambda}{\beta \cos \theta}$$

where D is the average crystal size, K Debye Scherrer's constant (= 0.94);  $\lambda$ , the wavelength of CuK $\alpha$  radiation (=0.154 nm);  $\beta$  is the angular full width half maximum (FWHM) of the XRD peak and  $\theta$ , the Bragg's diffraction angle. The average crystalline size of TiO<sub>2</sub> NPs synthesized by *G. glabra* was found to be ~69 nm.

This result corroborates with the previous studies of green synthesized TiO<sub>2</sub> nanoparticles and in good agreement with the standard data for TiO<sub>2</sub> nanoparticles. The diffraction peaks obtained were converted into d-spacing which is compared with the standard reference pattern of TiO<sub>2</sub>. The intensity of the diffraction peak of phytosynthesized TiO<sub>2</sub> is less when compared to chemically synthesized ones (Sharmila et al., 2014).

#### 3.4. Zeta potential ( $\zeta$ )

Stability of TiO<sub>2</sub> NPs was determined by Zeta potential measurements by means of the electrophoretic mobility ( $\mu$ ). A Zeta potential ( $\zeta$ ) of -31 mV was observed for TiO<sub>2</sub> NP stating that the particles were reasonably stable and dispersed evenly in the solvent at a given pH of 7. This decrease in zeta potential to more negative values for TiO<sub>2</sub> NPs

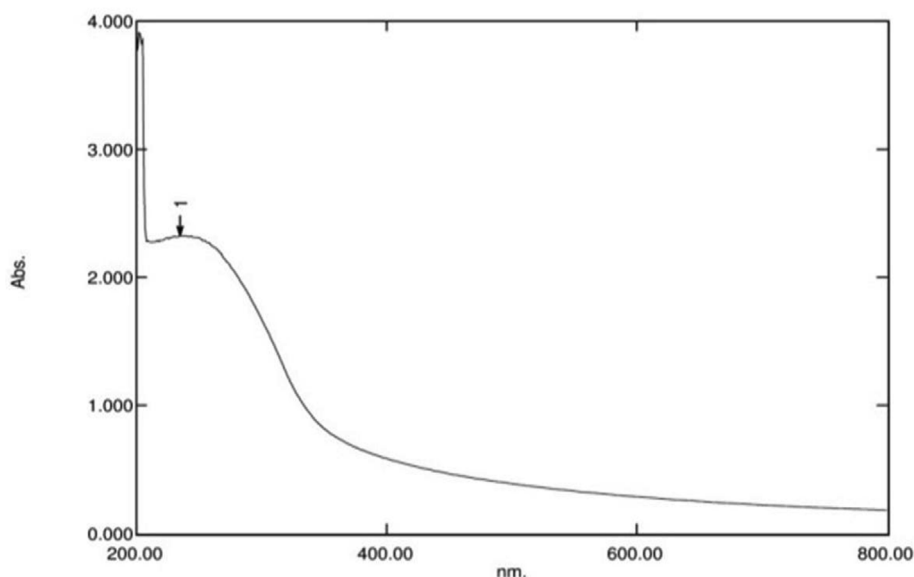


Fig. 1. UV Visible Spectrophotometric analysis of TiO<sub>2</sub>NPs.

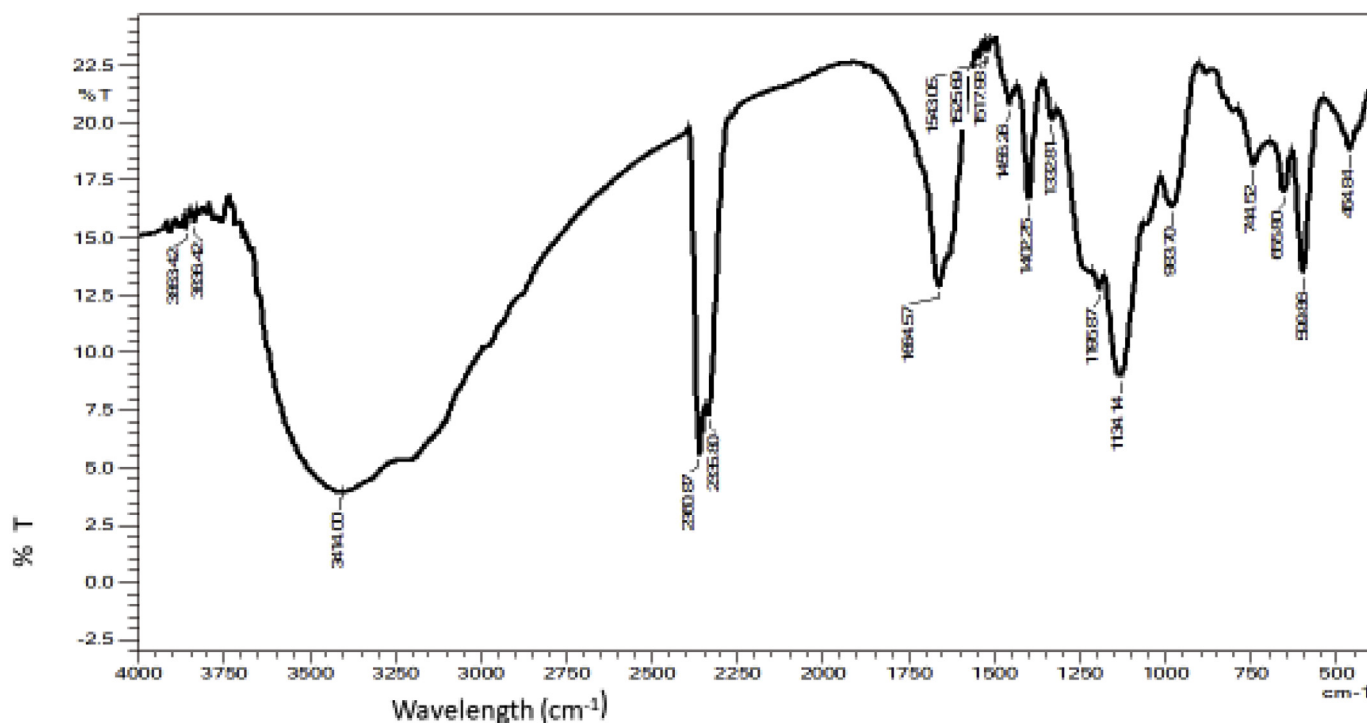


Fig. 2. FT-IR spectrum of TiO<sub>2</sub>NPs from *G. glabra* root extract.

with increasing pH could be due to the fact that the OH<sup>-</sup> concentration increased and thus bond with H<sup>+</sup> on the surface active sites of the TiO<sub>2</sub> NPs. As a result of this high negative value, there might be less possibility of aggregation of TiO<sub>2</sub> NPs in suspension (Romanello and Fidalgo de Cortalezzi, 2013).

### 3.5. FE-scanning electron microscopy

Fig. 3 shows the FESEM image of TiO<sub>2</sub> NPs synthesized using *G. glabra* root extract mediated. The micrographs revealed clear nanostructures with polydispersed grain size in the range of 60 nm–140 nm with spherical shape. It is known that the growth of colloids takes place by two mechanisms: dissolution of smaller and soluble particles followed by precipitation and growth of larger particles (Ostwald ripening) and secondly by agglomeration of smaller particles to form larger ones (Brinker and Scherer, 1990). We foresee that the latter mechanism might be involved in the growth of nanoparticles.

### 3.6. Antimicrobial activity of TiO<sub>2</sub> NPs

Nanomaterials divulge strong inhibiting effects towards a broad spectrum of bacterial strains. The microorganisms hold a negative

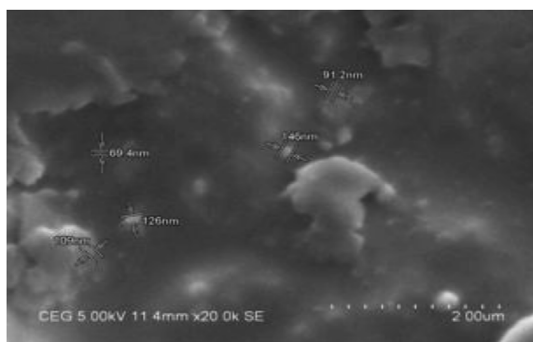


Fig. 3. SEM micrograph of TiO<sub>2</sub> NPs.

charge while the metal oxides transmit a positive charge. Hence, electrochemical attractions between microorganisms and the metal oxides lead to the oxidation and finally result in the death of microorganisms (archana et al., 2012). The agar diffusion method was adapted to test the antibacterial activity of TiO<sub>2</sub>NPs against *Staphylococcus aureus* and *Klebsiella pneumoniae*. The results suggest that there was a greater activity (as observed from ZOI) toward *Klebsiella pneumoniae* compared with the zones formed by plant extract (Fig. 4). The plant extract showed little or no activity against *Staphylococcus aureus* and *K. pneumoniae* whereas the nanoparticles showed potential antibacterial activity against the bacteria tested. When compared, there was a significant increase in the susceptibility towards Gram negative bacterium than Gram positive bacterium. It was believed that the germicidal mechanism of TiO<sub>2</sub> NPs involve release of positively charged ions and its adherence to the negatively charged thiol group (–SH) of the proteins on the cytoplasmic membrane (Jayaseelan et al., 2013). With the continued reaction, there is an increased permeability in the cell wall leading to deformation in the morphology of cellular components such as DNA, ribosomes and cellular enzymes and finally resulting in the

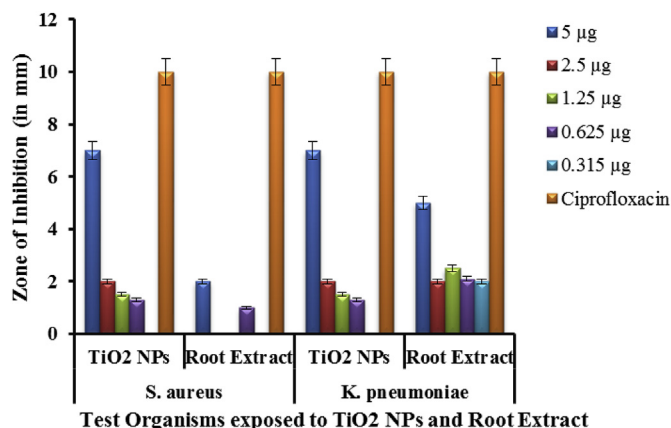


Fig. 4. Antibacterial activity of TiO<sub>2</sub> NPs and *G. glabra* root extract.

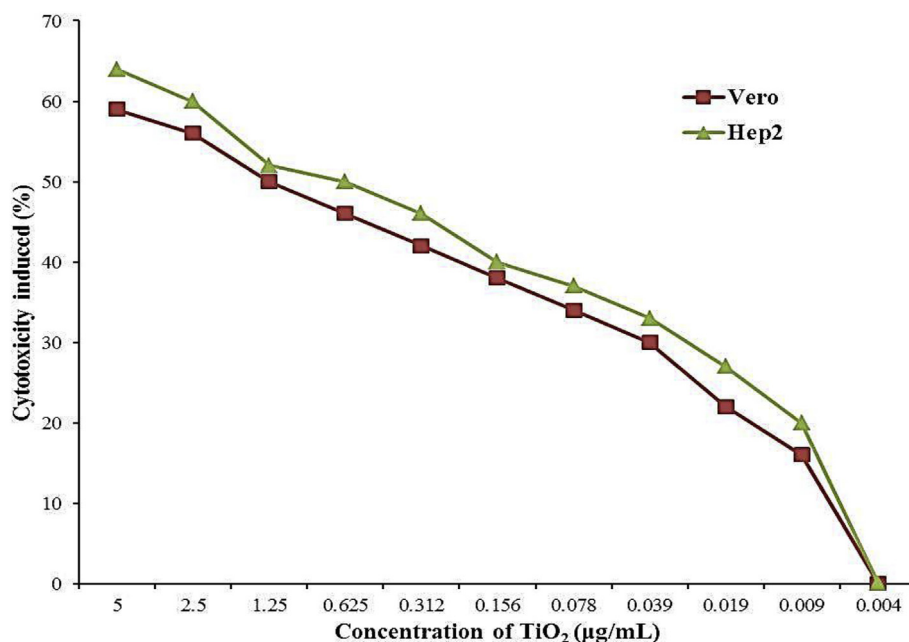


Fig. 5. Cytotoxicity study of Vero and HEp-2 cell lines exposed to various concentrations of TiO<sub>2</sub> NPs.

death of micro-organism (Koseki et al., 2009). Alongside, the photocatalytic activity of TiO<sub>2</sub> NPs might inactivate the microbial cells by interfering with the ion transport and disrupting the metabolic pathway.

### 3.7. Cytotoxicity studies

*In vitro* cytotoxicity of the TiO<sub>2</sub> NPs synthesized using *G. glabra* root extract was determined using MTT assay on Vero and HEp-2 cell lines at different concentrations (0.0045, 0.009, 0.0195, 0.039, 0.078, 0.156, 0.3125, 0.625, 1.25, 2.5 and 5 mg/ml) for 24 h. The TiO<sub>2</sub> NPs exhibited cell viability > 20% at highest concentration (5 mg/ml) and < 80% at lowest concentration as shown in Fig. 5. The IC<sub>50</sub> value of TiO<sub>2</sub> NPs against Vero and HEp-2 cells were found to be 1.25 µg and 0.3125 µg/ml respectively (Mosmann, 1983). Hence, from the study it was explained that TiO<sub>2</sub> NPs could selectively inhibit the growth of HEp-2 cells at 0.3125 µg/ml but were not toxic to Vero cell lines (Bavanilatha et al., 2016). It was proposed that the mechanism of cytotoxicity induced by TiO<sub>2</sub> NPs relies on the generation of reactive oxygen species (ROS). The oxidative stress induced by the TiO<sub>2</sub> NPs in turn induced significant generation of hydrogen peroxide and nitric oxide leading to oxidative DNA damage in the cells (Gurr et al., 2005) (see Fig. 5).

### 3.8. Biocompatibility studies of TiO<sub>2</sub> NPs using zebra fish model

The *in vivo* toxicity assay was performed with zebra fish embryos. Initially the fish eggs were fertilized externally. The embryos at different developmental stages were segregated and exposed to different concentrations of TiO<sub>2</sub> NPs (1, 0.5, 0.25, 0.125, 0.63 and 0.031 mg/ml) along with the control. The early embryonic stages viz. regular heart-beats, tail movements and blood flow movements were observed under the microscope. We found that almost all the embryos survived (80%) at lowest concentration (0.031 mg) and as the dosage increased, there was slight decline in survivability as the concentration increased. It was reported that TiO<sub>2</sub> NPs at a concentration upto 1 mg failed to induce major developmental malformations in zebra fish embryos (Wang et al., 2014). On the other hand, increase in concentration and its exposure for an extended period of time to such metal oxide nanoparticle would result in neurotoxicity (Chandrasekar, 2015; Zhao, 2013) and also lead to genotoxic effect (Rocco et al., 2015). There have also been reports on the adverse effect of TiO<sub>2</sub> NPs on the early embryonic development of zebrafish with malformed heads, cardiovascular issues, stunted growth and axial malformation. No such abnormalities were observed in our study where in TiO<sub>2</sub> NPs exposed embryos have shown growth on a par with the control embryos forecasting oblong, germ ring, somite and Pec fin stages (Fig. 6).

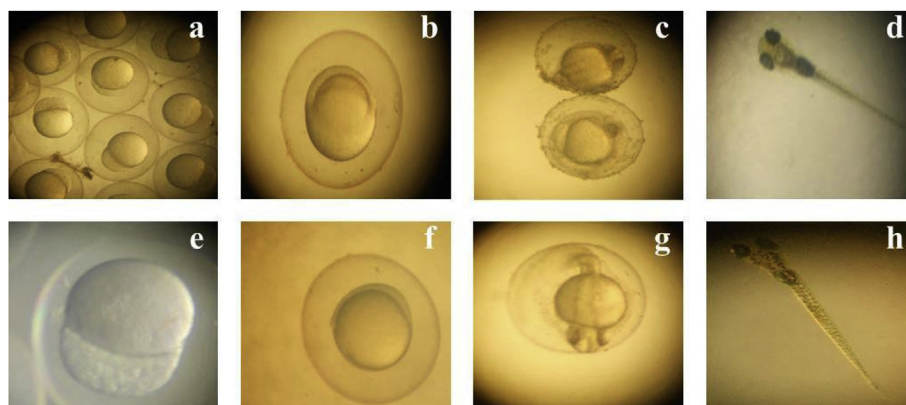


Fig. 6. Developmental stages of Zebra fish embryos (40 × Olympus) – Control (a–d) and TiO<sub>2</sub> NPs treated (e–h).

Developmental stages (a, e – Oblong stage; b, f – Germ ring; c, g – Somite stage; d, h – Pec fin stage).

#### 4. Conclusion

As the technological dependence in the recent years is on an increasing trend, there is a dire need for the lab scale research to move toward industry for uninterrupted demand-supply chain. In the present study, a novel approach in reducing TiOSO<sub>4</sub> to TiO<sub>2</sub> NPs using *G. glabra* plant extract has been attempted in an eco-benign fashion. TiO<sub>2</sub> NPs synthesized were characterized by using UV-vis spectrometer, XRD, FTIR and SEM which showed the typical nanocharacteristics. The antibacterial effect of TiO<sub>2</sub> NPs was found significant against *K. pneumoniae* and *S. aureus* with the ZOI more prominent in *K. pneumoniae* strain. The nanoparticles have tendency to form thiols revealed its counter-acting effect against bacteria. The *in vitro* study of TiO<sub>2</sub> NPs treated Vero and HEP-2 cells showed selective toxicity toward HEP-2 cells as determined using MTT assay. The *in vivo* study was carried out on zebra fish embryos to check its biocompatibility. TiO<sub>2</sub> NPs treated zebra fish embryos showed no distinctive malformations at all the embryonic stages proving its biocompatibility. There could be some control over the particle size which needs further optimization as the reduction in size would increase its biological efficiency to a greater extent. This could indeed provide us a lead for designing a multifaceted therapeutic agent to have its extended application in biomedical field.

#### Acknowledgement

The Authors would like to thank management of Sathyabama Institute of Science and Technology for providing the infrastructure facilities to undertake this research work.

#### Appendix A. Supplementary data

Supplementary data to this article can be found online at <https://doi.org/10.1016/j.bcab.2019.101131>.

#### References

- Archana, M., Pratima, C., Amita, M., Abay, K.P., 2012. Surface functionalization of TiO<sub>2</sub> with plant extracts and their combined antimicrobial activities against *E. faecalis* and *E. coli*. *J. Res. Updates Polym. Sci.* 1, 43–51.
- Balantrapu, K., Goia, D., 2009. Silver nanoparticles for printable electronics and biological applications. *J. Mater. Res.* 24, 2828–2834. <https://doi.org/10.1557/jmr.2009.0336>.
- Barbé, C.J., Arendse, F., Comte, P., Jirousek, M., Lenzmann, F., Shklover, V., Grätzel, M., 2005. Nanocrystalline titanium oxide electrodes for photovoltaic applications. *J. Am. Ceram. Soc.* 80 (12), 3157–3171.
- Bavanilatha, M., Yoshitha, L., Purnima, Ratnaprabha, 2016. Developmental toxicity of arsenic and its underlying mechanisms in the early embryonic development. *Res. J. Pharm. Technol.* 9 (4), 1–5.
- Bhainsa, K.C., D'Souza, S.F., 2006. Extracellular biosynthesis of silver nanoparticles using the fungus *Aspergillus fumigatus*. *Colloids Surf: Biointerfaces* 47, 160–164. <https://doi.org/10.1016/j.colsurfb.2005.11.026>.
- Blumenthal, M., Goldberg, B., 2000. Herbal medicine expanded C. monograph 58, 1685–1693.
- Brinker, C.J., Scherer, G.W., 1990. *Sol-Gel Science*. Academic Press, Boston.
- Chandrasekar, Shanmugam, Chandrasekaran, Chandramouli, Muthukumarasamyvel, Thangavel, Sudhandiran, Ganapasam, Rajendiran, Nagappan, 2015. Sodium cholate–Templated Blue light emitting Ag sub nanoclusters: in vivo toxicity and imaging in zebrafish embryos. *ACS Appl. Mater. Interfaces* 7 (3), 1422–1430.
- Ching-song, J., Der-chi, T., Tun-Ping, T., Ho, Chang, Tsing-Tshih, T., Chih-Yu, L., Chi-Hsiang, L., 2005. Preparation and UV characterization of TiO<sub>2</sub> nanoparticles synthesized by SANSS. *Rev. Adv. Mater. Sci.* 10, 283–288.
- Dongxu, Z., Zhaoxia, J., Xingmao, J., Darren, R.D., Jeffrey, B., Arturo, A.K., 2013. Influence of material properties on TiO<sub>2</sub> nanoparticle agglomeration. *PLoS One* 8 (11).
- Esra, Ibanoglu, Senol, Ibanoglu, 2000. Foaming behaviour of liquorice (*Glycyrrhiza glabra*) extract. *Food Chem.* 70 (3), 333–336.
- Gupta, M., Gupta, A.K., 2004. *In vitro* cytotoxicity studies of hydrogel pullulan nanoparticles prepared by AOT/N-hexane micellar system. *J. Pharm. Pharmaceutical Sci.* 7 (1), 38–46.
- Gurr, J.R., Wang, A.S., Chen, C.H., Jan, K.Y., 2005. Ultrafine titanium dioxide particles in the absence of photoactivation can induce oxidative damage to human bronchial epithelial cells. *Toxicology* 213 (1–2), 66–73.
- Hudlikar, M., Joglekar, S., Dhaygude, M., Kodam, K., 2012. Green synthesis of TiO<sub>2</sub> nanoparticles by using aqueous extract of *Jatropha curcas* L latex. *Matt. Lett.* 75, 196–199.
- Jayaseelan, C., Rahuman, A.A., Roopan, S.M., Kirthi, A.V., Venkatesan, J., Kim, Iyappan, M., Siva, C., 2013. Biological approach to synthesize TiO<sub>2</sub> nanoparticles using *Aeromonas hydrophila* and its antibacterial activity. *Spectrochim. Acta Mol. Biomol. Spectrosc.* 107, 82–89. <https://doi.org/10.1016/j.saa.2012.12.083>.
- Khare, 2007. *Indian Medicinal Plants-Books an Illustrated Dictionary*.
- Koseki, H., Shiraiishi, K., Asahara, T., Tsurumoto, T., Shindo, H., 2009. Photocatalytic bactericidal action of fluorescent light in a titanium dioxide particle mixture: an *in vitro* study. *Biomed. Res.* 30, 189–192.
- Kong, J.-Z., Li, A.-D., Li, X.-Y., Zhai, H.-F., Zhang, W.-Q., Gong, Y.-P., Li, H., Wu, D., 2010. *J. Solid State Chem.* 183, 1359–1364.
- Kreyling, W.G., Semmler, M., Erbe, F., Mayer, P., Takenaka, S., Schulz, H., Oberdörster, G., Ziesenis, A., 2002. Translocation of ultrafine insoluble iridium particles from lung epithelium to extrapulmonary organs is size dependent but very low. *J. Toxicol. Environ. Health* 65A, 1513–1530.
- Mosmann, T., 1983. Rapid colorimetric assay for cellular growth and survival: application to proliferation and cytotoxicity assays. *J. Immunol. Methods* 65, 55–63.
- Mukherjee, P., Ahmad, A., Mandal, D., Senapati, S., Sainkar, S.R., 2001. Fungus-mediated synthesis of silver nanoparticles and their immobilization in the mycelial matrix: a novel biological approach to nanoparticle synthesis. *Nano Lett.* 1, 515–519. <https://doi.org/10.1021/nl0155274>.
- Murugan, A.V., Samuel, V., Ravi, V., 2006. Synthesis of nanocrystalline anatase TiO<sub>2</sub> by microwave hydrothermal method. *Mater. Lett.* 60, 479–480. <https://doi.org/10.1016/j.matlet.2005.09.017>.
- Paskalis, S.M.K., Francis, Arul, P., Thiyagarajan, D., 2014. Biosynthesized and chemically synthesized Titania Nanoparticles: comparative analysis of antibacterial activity. *J. Environ. Nanotechnol.* 3 (3), 73–81.
- Rajakumar, Govindasamy, Abdul, Chidambaram, et al., 2013. *Solanum trilobatum* extract-mediated synthesis of titanium dioxide nanoparticles to control *Pediculus humanus capitis*, *Hyalomma anatolicum anatolicum* and *Anopheles subpictus*. *Parasitol. Res.* 113. <https://doi.org/10.1007/s00436-013-3676-9>.
- Rajakumar, G., Rahuman, A.A., Priyamvada, B., Khanna, V.G., Kumar, D.K., Sujin, P.J., 2012. *Eclipta prostrata* leaf aqueous extract mediated synthesis of titanium dioxide nanoparticles. *Mater. Lett.* 68, 115–117.
- Rocco, L., Santonastaso, M., Mottola, F., Costagliola, D., Suero, T., Pacifico, S., Stingo, V., 2015. Genotoxicity assessment of TiO<sub>2</sub> nanoparticles in the teleost *Danio rerio*. *Ecotoxicol. Environ. Saf.* 113, 223–230.
- Romanello, M.B., Fidalgo de Cortalezzi, M.M., 2013. An experimental study on the aggregation of TiO<sub>2</sub> nanoparticles under environmentally relevant conditions. *Water Res.* 47 (12), 3887–3898.
- Shashank Chetty, S., Praneetha, S., Basu, Sandeep, Sachidanandan, Chetana, Vadivel murugan, A., 2016. Sustainable, Rapid Synthesis of Bright –Luminescent CuInS<sub>2</sub>-ZnS Alloyed Nanocrystals; Multistage Nano-Xenocytotoxicity Assessment and Intravital Fluorescence Bioimaging in Zebra Fish –Embryos. *Scientific Reports*. [www.nature.com](https://www.nature.com).
- Sharmila, D., Venkatesh, Rajeshwari, Sivaraj, 2014. Synthesis of titanium dioxide nanoparticles by sol-gel technique. *Int. J. Innov. Res. Sci. Eng. Technol.* 3 (8), 15206–15211. <https://doi.org/10.15680/IJRSET.2014.0308020>.
- Swetha, S., Valli, N., Rashmi, L., Renugadevi, 2014. Biogenesis of TiO<sub>2</sub> Nanoparticles using endophytic *Bacillus cereus*. *J. Nano Res.* 16, 2681.
- Taleb, A., Petit, C., Pilen, M.P., 1997. Synthesis of highly monodisperse silver nanoparticles from AOT reverse micelles: a way to 2D and 3D self-organization. *Chem. Mater.* 9 (4), 950–959. <https://doi.org/10.1021/cm960513y>.
- Valli, N., Vijayalakshmi, R., Nivedha, K., Bavanilatha, M., Swetha, S., 2016. *Moraxella osloensis* mediated synthesis of TiO<sub>2</sub> nanoparticles. *Int. J. Pharm. Pharm. Sciences* 8 (5), 397–400.
- Wang, Y.J., He, Z.Z., Fang, Y.W., Xu, Y., Chen, Y.N., Wang, G.Q., Yang, Y.Q., Yang, Z., Li, Y.H., 2014. Effect of titanium dioxide nanoparticles on zebrafish embryos and developing retina. *Int. J. Ophthalmol.* 7, 917–923.
- Willner, I., Basnar, B., Willner, B., 2007. Nanoparticle–enzyme hybrid systems for nanobiotechnology. *FEBS J.* 274, 302–309. <https://doi.org/10.1111/j.1742-4658.2006.05602>.
- Zhao, X., Wang, Shutao, Wu, Yuwan, Hong, 2013. Acute ZnONPs exposure induces developmental toxicity, oxidative stress and DNA damage in embryo larval zebrafish. *Aquat. Toxicol.* 136, 49–59.